

Strongly First Order Phase Transitions Near an Enhanced Discrete Symmetry Point

Vernon Barger,^a Daniel J. H. Chung,^a Andrew J. Long,^a and Lian-Tao Wang^b

^a*Department of Physics, University of Wisconsin, Madison, WI 53706*

^b*Enrico Fermi Institute and Department of Physics, University of Chicago, Chicago, IL 60637*

E-mail: barger@pheno.wisc.edu, danielchung@wisc.edu, ajlong@wisc.edu,
liantaow@uchicago.edu

ABSTRACT: We propose a group theoretic condition that can be used for locating the parametric regions in extensions of the Standard Model which display a strongly first order phase transition necessary for electroweak baryogenesis. Specifically, we demonstrate that an arbitrarily strong phase transition can be found near an enhanced discrete symmetry point in the parameter space if the condition for spontaneous symmetry breaking is met and if the discrete symmetry relates the electroweak symmetry preserving vacuum and the one where it is broken. This idea is used to investigate several specific models of the electroweak symmetry breaking sector. The phase transitions identified through this method suggest implications for other relics such as dark matter and gravitational waves.

KEYWORDS: electroweak phase transition, beyond the Standard Model

Contents

1	Introduction	1
2	Why Discrete Symmetry?	3
3	A Few Examples	6
3.1	SM with Low Cutoff	6
3.2	SM Plus Real Singlet – xSM	8
3.3	SM Plus Real \mathbb{Z}_2 -Charged Singlet – \mathbb{Z}_2 xSM	10
4	Conclusion	12
A	Details of Phase Transition Calculation	12

1 Introduction

Standard cosmology of the early universe within the context of a large class of models embedding the Standard Model (SM) of particle physics predicts the existence of an electroweak symmetry breaking (EWSB) phase transition (PT). Collider constraints alone cannot determine the nature of the EWSB PT in a model independent way. However, additional information is available in the form of cosmological relics, which were produced in the early universe and survive as direct probes of the physics of the era during which the temperature was electroweak scale. Relics such as the baryon asymmetry [1], primordial gravitational waves [2–5], and (modifications to) the dark matter relic abundance [6–9], may have been generated at the electroweak scale PT(s).

Generating the baryon asymmetry through CP violations at electroweak symmetry breaking bubbles [1], requires a strongly first order phase transition (SFOPT) to protect the baryon number in the broken phase. In this context, a SFOPT may be defined as a first order PT in which the (thermal) expectation value of the SM-like Higgs $v(T) = \langle h \rangle$ satisfies $v(T)/T \gtrsim 1$ in the broken phase after the phase transition completes, such that weak sphaleron processes are inactive [1, 10]. It is well-known that the SM is unable to accommodate a SFOPT while satisfying the Large Electron-Positron (LEP) Collider bounds on the Higgs mass [11]. This is one of the main motivations for considering an extended Higgs sector. Many beyond the Standard Model theories are able to accommodate a SFOPT, including supersymmetry, two Higgs doublet models, and minimal scalar singlet extensions of the SM. However, if the extra scalar fields obtain vacuum expectation values (vevs), one often finds that new patterns of symmetry breaking become accessible. This fact makes the phase transition more difficult to study, because quantities such as $v(T)/T$ are nonanalytic functions of the parameters of the model. To illustrate this point, consider

a scenario in which the PT may proceed directly from an EW-preserving vacuum **A** to an EW-breaking vacuum **C** or alternatively from **A** to an intermediate vacuum **B** (in which some other symmetry may be broken) and then subsequently to **C**. As some model parameter λ is varied to make the **A** to **C** transition more strongly first order, it may happen that once a threshold is crossed $\lambda > \lambda_c$ the **A** to **B** to **C** transition becomes active instead. In this way, an extended Higgs sector may accommodate a SFOPT and generate a richer phase transition structure, but at the same time, the additional degrees of freedom make the PT more difficult to study analytically. Consequently, many beyond the Standard Model PT analyses rely on an intensive numerical parameter scan to search for SFOPT. Although such scans may be capable of locating SFOPTs, on their own they do not reveal why one particular parametric limit is favored over another.

In this article, we propose a group theoretic guideline which will aid the search for SFOPT in a large parameter space and help to identify why certain parametric limits are favored over others. Our guideline is motivated by the following heuristic argument. In perturbative thermal effective potential computations, the thermal mass is of the order cT^2 where c is a thermal loop factor. Therefore, if all the renormalized coupling constants are of order unity and all mass scales are of the electroweak scale, we expect that the phase transition will occur at a temperature $T \sim v/\sqrt{c}$ such that $v(T)/T \sim \sqrt{c} < 1$, and the PT is typically not strongly first order. Hence, in order to have a SFOPT, the renormalized parameters of the theory must be near a special point in the parameter space. An ideal parametric limit which overcomes the natural thermal loop suppression is the region where $v(T)/T \rightarrow \infty$. To achieve this, it would be unnatural to expect $v(T)$ to deviate by many orders of magnitude from the electroweak scale, because of the constraint that $v(0)$ defines the electroweak scale. On the other hand, a low temperature phase transition can be achieved naturally. For concreteness, we may evaluate the criterion $v(T)/T > 1$ at the representative phase transition temperature T_c , defined as the temperature at which the thermal effective potential possesses two degenerate minima (see also Appendix A). Then, one may take $T_c \rightarrow 0$ provided that there is a mechanism guaranteeing that the theory possesses degenerate vacua even in the absence of thermal corrections.

One mechanism for generating such degenerate vacua is to have spontaneous symmetry breaking of a discrete symmetry (see e.g. [12, 13]) which does not commute with the electroweak group. Such spontaneous breaking leads to the set of degenerate vacua realizing a coset representation of the discrete symmetry. The noncommuting requirement guarantees that a transition between two vacua related by the discrete symmetry can be responsible for EWSB if one of the coset representation elements is an electroweak singlet. The simplest example of a discrete symmetry satisfying these requirements, is a \mathbb{Z}_2 which relates an electroweak symmetry preserving vacuum to one which breaks the electroweak symmetry. After spontaneous symmetry breaking, the discrete symmetry will be completely broken.

To sum up our group theoretic guideline, if at a particular parametric point, referred to as an enhanced discrete symmetry point (EDSP), the theory admits a discrete symmetry which relates EW-preserving with EW-broken vacua, then one can expect to find SFOPT in a parametric region which is connected to the EDSP by a continuous “small” deformation which breaks the discrete symmetry. Precisely how “small” a deformation is required

depends upon two model-dependent conditions: the condition that the electroweak PT must complete, because if the discrete symmetry is not sufficiently broken then nucleation of EW-broken bubbles can not take place, and upon the the order unity number that sits at the right of the inequality $v(T)/T > 1$. It is not unnatural to expect SFOPT to be localized in the vicinity of an EDSP. Strongly first order phase transitions almost always requires some fine-tuning of the parameters in the theory. From an UV completion point of view, such fine-tuning could be more natural if it is close to a point of the parameter space with enhanced symmetry. One may alternatively consider utilizing an enhanced continuous symmetry point to identify SFOPT, however the discrete symmetry limit is more natural from the desire to achieve $v(T)/T \rightarrow \infty$ for a *first order* PT since the degenerate vacua will be separated by a potential barrier. Finally, it is clear that degenerate vacua may be found even without discrete symmetry, and thus our guideline provides a sufficient, though not necessary, condition for locating SFOPT. Nonetheless, such parametric regions form a large class of possibilities which can almost always occur in practice.

The order of presentation is as follows. In Sec. 2 we motivate our group theoretic identification of SFOPTs. In Sec. 3, we employ our technique to explore three example models. We then finish with some concluding remarks in Sec. 4 and an appendix which reviews some relevant basics of phase transitions used in this paper.

2 Why Discrete Symmetry?

Suppose that a given theory is exactly invariant under an internal discrete symmetry group G . It is well-known that the spontaneous symmetry breaking of G down to $H \subset G$ leads to the vacua giving a nontrivial coset G/H representation [12, 13]. We will first illustrate how this connects to a SFOPT in a perturbative single real scalar field toy model, and then proceed to give a more general discussion.

Consider the theory of a real scalar field φ with the classical potential

$$U(\varphi) = \frac{1}{2}M^2\varphi^2 - \mathcal{E}\varphi^3 + \frac{\lambda}{4}\varphi^4, \quad (2.1)$$

and suppose that φ is coupled to a family of N fermions $\mathcal{L} \supset h_i\varphi\bar{\psi}_i\psi_i$. Note that this theory has no internal symmetries for non-special values of the parameters $\{M^2, \mathcal{E}, \lambda, h_i\}$. When we turn on temperature, there will be a thermal bath of φ and ψ_i particles. If the fermions are relativistic at the electroweak scale, then the thermal effective potential can be written to leading order as

$$V_{\text{eff}}(\varphi, T) \approx U(\varphi) + cT^2\varphi^2 \quad (2.2)$$

where $c \approx Nh_i^2/12$. Here, in the so-called high-temperature approximation, we have neglected the subdominant thermal and \hbar radiative corrections.

As long as the supercooling is small (e.g., as measured by the fractional temperature change during the duration of the PT), the PT occurs at the temperature near T_c at which the thermal effective potential V_{eff} displays two degenerate minima (for more details, see

Sec. A). Solving this constraint for T_c gives

$$T_c^2 = \frac{\mathcal{E}^2}{\lambda c} \left(1 - \frac{\lambda M^2}{2\mathcal{E}^2} \right). \quad (2.3)$$

In this simple toy model and subject to the approximation Eq. (2.2), there is an enhanced \mathbb{Z}_2 symmetry at $T = T_c$. Explicitly, the potential at $T = T_c$ becomes

$$V_{\text{eff}}(\varphi, T_c) = \frac{\lambda\varphi^2}{4} \left(\varphi - \frac{2\mathcal{E}}{\lambda} \right)^2, \quad (2.4)$$

which is notably independent of M . The resulting discrete symmetry,

$$\mathbb{Z}_2 : \left(\varphi - \frac{\mathcal{E}}{\lambda} \right) \rightarrow - \left(\varphi - \frac{\mathcal{E}}{\lambda} \right), \quad (2.5)$$

exchanges the degenerate vacua at $\varphi = 0$ and $\varphi = v(T_c) = 2\mathcal{E}/\lambda$ across a potential barrier at $\varphi = \mathcal{E}/\lambda$. It is to be noted that this symmetry exists in this toy model for any critical temperature T_c that can be tuned using M .

Although there is no electroweak symmetry in this toy model, there is still a first order phase transition, and we can investigate the parametric dependence of its order parameter $v(T_c)/T_c$. Since $v(T_c) = 2\mathcal{E}/\lambda$ is independent of M^2 , the order parameter can be maximized by varying M^2 to minimize T_c . Even though the high-temperature expansion breaks down when T drops below the mass of the fermion, the formal limit $T_c \rightarrow 0$ can be taken assuming that the fermions are massless. The formal solution to $T_c = 0$ is¹

$$\alpha \equiv \lambda M^2 / 2\mathcal{E}^2 = 1. \quad (2.6)$$

The important observation is that $1 - \alpha = 0$ corresponds to an EDSP in the parameter space at which the *zero-temperature* scalar potential Eq. (2.1) is invariant under the symmetry transformation Eq. (2.5). At the EDSP, $1 - \alpha = 0$, the order parameter

$$\frac{v(T_c)}{T_c} = 2\sqrt{\frac{c}{\lambda}} \frac{1}{\sqrt{1 - \alpha}} \quad (2.7)$$

formally diverges, and for $1 - \alpha \ll 1$, the phase transition may be made arbitrarily strongly first order.

Hence, our group theoretic guideline leads us to identify the parametric region in the vicinity of the EDSP $1 - \alpha = 0$ as favorable for SFOPT. However, for this region to be truly viable, it must be the case that the rate at which bubbles of the broken phase nucleate is sufficiently large that the phase transition actually completes. This requires the discrete symmetry to be weakly broken, such that the PT occurs at a nonzero T .² In the toy model, such breaking can be accomplished explicitly at the classical level through a finite excursion from the EDSP (i.e. $1 - \alpha = \epsilon \neq 0$), or radiatively through the Yukawa coupling. Indeed, in many extensions of the SM where singlets are introduced, the relevant discrete symmetry

¹ The idea of focusing on $T_c \approx 0$ was recently emphasized by [14].

²Note that the bubble nucleation rate in zero at $T = T_c$.

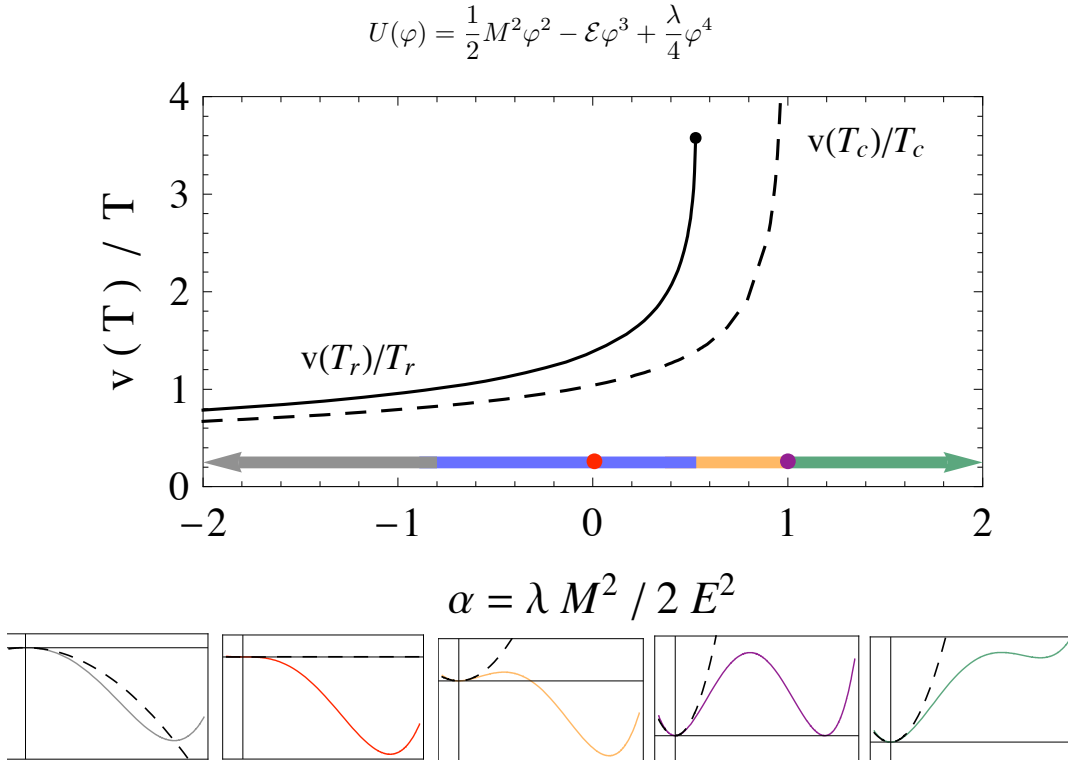


Figure 1. The order parameter, calculated as $v(T_c)/T_c$ (dashed) and $v(T_r)/T_r$ (solid), plotted against $\alpha = \lambda M^2/2E^2$. The insets show $U(\varphi)$ for particular values of α in each of the associated colored regions.

transforms both the Higgs and the singlet fields. Since the singlets lack SM gauge couplings, radiative corrections necessarily break the discrete symmetry to a degree controlled by the strength of the gauge interactions. If the breaking of the symmetry is too large, the benefit of the EDSP method proposed here in identifying a SFOPT is lost. If the breaking of the symmetry is too small, then the bubbles will not nucleate fast enough to complete the PT. Since this non-completion of the PT will be a general feature of the region of parameter space nearby to the EDSP, we must take extra care in choosing the temperature at which to evaluate the EW order parameter $v(T)/T$. The order parameter specified above, $v(T_c)/T_c$, can be calculated independent of whether or not the PT completes. We will additionally evaluate the more physically relevant quantity $v(T_r)/T_r$ where T_r is the temperature in the broken phase after reheating, which does not exist if the PT does not complete.

To obtain a numerical intuition for our proposal, consider Fig. 1 where we have plotted $v(T_c)/T_c$ (dashed) and $v(T_r)/T_r$ (solid) while varying α and fixing $U'(v) = 0$ at $v = 300 \text{ GeV}$, $U''(v) = (50 \text{ GeV})^2$, $N = 1$, and $h = 0.3$. In this figure, we also show $U(\varphi)$, such as to make the discrete symmetry evident at the EDSP. As expected, $v(T_c)/T_c$ diverges at the EDSP and is arbitrarily large for arbitrarily small discrete symmetry breaking ($1 - \alpha \ll 1$). On the other hand, $v(T_r)/T_r$ cannot be calculated if the discrete symmetry is too weakly broken ($1 - \alpha \lesssim 0.5$), because the phase transition does not occur. However, sufficient

discrete symmetry breaking ($1 - \alpha \gtrsim 0.5$) yields SFOPT which become monotonically weaker as the degree of symmetry breaking grows. We have used the same coloring in Fig. 1 as we do in the rest of this article to distinguish the various regions of parameter space: the phase transition does not occur because the broken phase is not energetically favored (green); the PT does not occur because the bubble nucleation rate is too low (orange); a strongly first order PT occurs (blue); a weakly first order or second order PT occurs (gray); the EDSP (purple dot); and the point at which the barrier disappears (red dot).

Now let us return to a more broad discussion of the connection between discrete symmetry and strongly first order phase transition. In retrospect, we recognize that the existence of an EDSP associated with a discrete symmetry under which the vacua form a coset representation (along with the condition that spontaneous symmetry breaking occurs) is sufficient to obtain $v(T_c)/T_c \rightarrow \infty$ since $T_c = 0$ implies a degeneracy at the level of the non-thermal effective potential. Even though the toy model calculation was accomplished using the leading high-temperature T dependence and the classical potential, this statement regarding the EDSP is an exact statement for an exact effective potential. In other words, as far as this exact statement is concerned, it is not particularly important that $T = T_c$ corresponded to an enhanced symmetry point for general T_c as in the case of this simple one dimensional toy model (see Eq. (2.4)), nor is it important that quantum radiative corrections from the Yukawa couplings break the discrete symmetry given by Eq. (2.5). One final ingredient, which is important for electroweak baryogenesis but is not represented in the toy model is that at least two vacua in the coset space must carry different electroweak quantum numbers. Otherwise, the PT will not be an electroweak symmetry breaking PT. This means that the discrete group must not commute with the electroweak group and one element in the coset representation must be an electroweak singlet. Hence our proposal, by which one may locate SFOPT with the aid of an EDSP “lamppost,” can be stated as follows: an arbitrarily strong PT can be found for parameters near an EDSP if the condition for its spontaneous symmetry breaking is met at $T = 0$ and if the coset representation containing an electroweak singlet element does not commute with the electroweak group.

3 A Few Examples

3.1 SM with Low Cutoff

As a first example, we will consider a generic extension of the SM with a low scale cutoff, as studied by [15–17]. Provided that the UV physics does not violate the EW symmetry, then upon integrating it out one obtains a classical potential of the form

$$-\mathcal{L} \supset \lambda \left(|H^\dagger H| - \frac{v^2}{2} \right)^2 + \frac{1}{\Lambda^2} \left(|H^\dagger H| - \frac{v^2}{2} \right)^3 \quad (3.1)$$

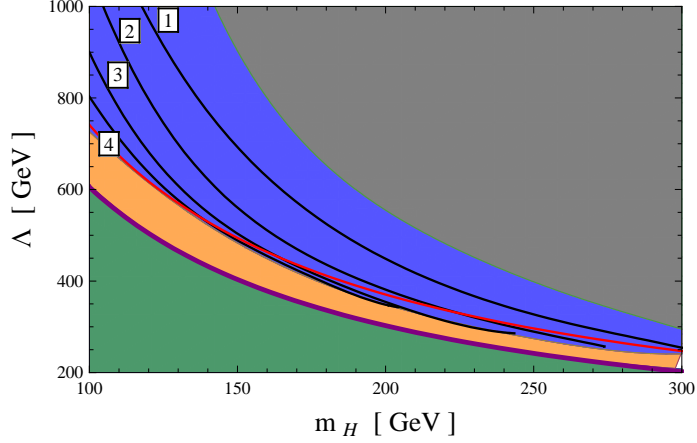


Figure 2. The parameter space nearby to the EDSP (purple curve). The coloring is the same as in Fig. 1. The PT order parameter $v(T_r)/T_r$ is indicated by the overlaid contours. SFOPTs are found in the blue region and become weaker in the gray region, farther from the EDSP.

up to terms of order H^8/Λ^4 . Writing the Higgs doublet in terms of the fundamental scalar Higgs h as $H = (0, h/\sqrt{2})^T$, and using $m_H^2 = 2\lambda v^2$, the potential becomes

$$U(h) = \frac{1}{8\Lambda^2} h^6 - \frac{\lambda}{4} \left(3 \frac{v^4}{m_H^2 \Lambda^2} - 1 \right) h^4 + \frac{\lambda v^2}{4} \left(3 \frac{v^4}{m_H^2 \Lambda^2} - 2 \right) h^2 \quad (3.2)$$

up to constant and higher order terms. There exists an enhanced discrete symmetry point³ at which a \mathbb{Z}_2 symmetry is nonlinearly realized,

$$\text{EDSP : } m_H \Lambda = v^2 \quad \mathbb{Z}'_2 : h \rightarrow -\frac{h}{2} + \sqrt{v^2 - \frac{3}{4}h^2}. \quad (3.3)$$

The \mathbb{Z}'_2 symmetry exchanges the minima at $h = 0$ and $h = v$ while leaving the maximum at $h = v/\sqrt{3}$ invariant. We have reproduced an earlier PT analysis [15] in order to illustrate the proximity of SFOPTs to the EDSP. Moreover, we have extended the previous analysis by calculating the more physically relevant order parameter $v(T_r)/T_r$, instead of $v(T_c)/T_c$. Our results are summarized in Fig. 2, and are in good agreement with Fig. 2 of [15] which shows the same slice of parameter space. We find that nearby to the EDSP (purple curve), the PT is strongly first order (blue), and that the PT becomes weaker moving away from the EDSP. It is also worth noting that while the barrier persists, the PT most likely does not occur, as evidenced by the lack of blue in the region between the purple and red curves except for a small sliver above $m_H = 200$ GeV.

³It may be more appropriate to use the term “enhanced discrete symmetry plane,” as the condition $m_H \Lambda = v^2$ actually specifies a hypersurface in the parameter space, but we will continue using EDSP for simplicity.

3.2 SM Plus Real Singlet – xSM

Next, we will consider models with multiple scalars in the electroweak sector. Extending the SM by a real scalar singlet s , we obtain a model known as the xSM [18], which has the classical potential

$$U(h, s) = \frac{\lambda_0}{4}h^4 - \frac{\mu^2}{2}h^2 + \frac{b_4}{4}s^4 + \frac{b_3}{3}s^3 + \frac{b_2}{2}s^2 + \frac{a_2}{4}s^2h^2 + \frac{a_1}{4}sh^2. \quad (3.4)$$

Since there is no symmetry protecting $s = 0$, generally both h and s will obtain vevs, denoted v and x_0 respectively, and the mass parameters may be written as

$$\mu^2 = \lambda_0 v^2 + \frac{a_2}{2}x_0^2 + \frac{a_1}{2}x_0 \quad \text{and} \quad b_2 = -b_4x_0^2 - b_3x_0 - \frac{a_2}{2}v^2 - \frac{a_1}{4}\frac{v^2}{x_0}. \quad (3.5)$$

Provided that $x_0 \neq 0$, the cubic terms s^3 and sh^2 help to generate a barrier separating the symmetric and broken vacua and make the PT strongly first order. A number of PT analyses [14, 19–21] have revealed that the xSM can accommodate a strongly first order electroweak PT. They also find that this model displays multiple patterns of symmetry breaking such that, either h and s can obtain vevs at the same temperature, or s can receive a vev prior to electroweak symmetry breaking. If we were to search for SFOPT by randomly choosing order one parameters, there would be no way of anticipating what pattern of symmetry breaking would be realized, or if the EW symmetry would be spontaneously broken at all. Moreover, since Eq. (3.4) has six free parameters, a such a random search could become quite time consuming.

The discrete symmetry technique greatly simplifies the SFOPT search. We are able to specify a desired pattern of symmetry breaking to investigate, identify the corresponding discrete symmetry, compute the associated EDSP, and begin searching by perturbing from the EDSP. Here, we will focus on a particular pattern of symmetry breaking in which both s and h obtain vevs simultaneously, and we will compare our calculation against the “high-T trivial singlet vev” case of [19]. The appropriate discrete symmetry is a \mathbb{Z}_2 relating the vacua at $\{h, s\} = \{0, 0\}$ and $\{v, x_0\}$. We can identify the associated EDSP by first reducing Eq. (3.4) to Eq. (2.1) and then imposing $\alpha = 1$. This is accomplished by focusing on the one-dimensional linear trajectory $\{h, s\} = \varphi \{v, x_0\} / \sqrt{v^2 + x_0^2}$, which interpolates between the EW-symmetric and EW-broken vacua. Along this trajectory, the potential can be written in the form of Eq. (2.1) with

$$\begin{aligned} \lambda &= \frac{\lambda_0 v^4 + b_4 x_0^4 + a_2 v^2 x_0^2}{(v^2 + x_0^2)^2} & \mathcal{E} &= -\frac{x_0(3a_1 v^2 + 4b_3 x_0^2)}{12(v^2 + x_0^2)^{3/2}} \\ M^2 &= \sqrt{v^2 + x_0^2} \left(3\mathcal{E} - \lambda \sqrt{v^2 + x_0^2} \right) & \alpha &= \frac{\lambda M^2}{2\mathcal{E}^2}. \end{aligned} \quad (3.6)$$

Then, upon resolving the condition $\alpha = 1$ we find the enhanced discrete symmetry point,

$$\begin{aligned} \text{EDSP : } & 0 = 12a_2 v^2 x_0^2 + 3a_1 v^2 x_0 + 4b_3 x_0^3 + 12b_4 x_0^4 + 6\lambda_0 v^4 \\ \mathbb{Z}_2 : & \left(\varphi - \frac{\mathcal{E}}{\lambda} \right) \rightarrow -\left(\varphi - \frac{\mathcal{E}}{\lambda} \right). \end{aligned} \quad (3.7)$$

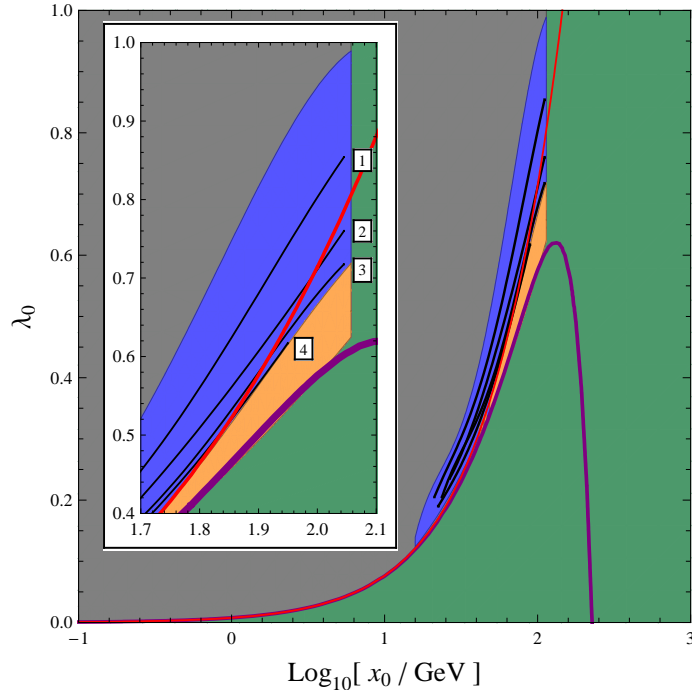


Figure 3. A slice of the xSM parameter space showing the proximity of SFOPT (blue region) to the enhanced symmetry axis (purple curve).

In general, the PT will not occur along the trajectory parameterized by φ , but nevertheless this linear interpolation is useful for identifying the EDSP.

Once again, we have numerically investigated the strength of first order PTs in the vicinity of the EDSP. We have chosen a parameter set which allows us to reproduce Fig. 4 (left panel) of [19] by fixing $a_1 = -933$ GeV, $a_2 = 0.69$, $b_3 = 356$ GeV, $b_4 = 0.53$ and scanning $\lambda_0 \in [0, 1]$ and $\log_{10} x_0 \in [-1, 3]$. Our results are shown in Fig. 3. A few observations may be made. First, as anticipated, the first order PTs are strongest close to the EDSP (purple) curve and become weaker farther away. Second, there is a large region (green) in which the EW remains unbroken. Below the EDSP (purple) curve, the origin remains the global minimum of the effective potential, whereas at large values of $x_0 \gtrsim 10^{2.1}$, the global minimum sits at $s < 0$. Third, in comparing with [19], one must bear in mind that we have fixed the remaining parameters, whereas those authors have scanned the full parameter space and projected onto these coordinates. As such, the region where we find SFOPT is much smaller than what is suggested by Fig. 4 of [19]. However, this just goes to show that it is typically difficult to find SFOPT in a large parameter space without either a large parameter scan or some guiding principle.

3.3 SM Plus Real \mathbb{Z}_2 -Charged Singlet – \mathbb{Z}_2 xSM

As a final example, we turn our attention to the \mathbb{Z}_2 xSM, which extends the SM by a real scalar singlet s such that the scalar potential becomes [14, 22]

$$U(h, s) = \frac{\lambda}{4}h^4 - \frac{\mu^2}{2}h^2 + \frac{b_4}{4}s^4 + \frac{b_2}{2}s^2 + \frac{a_2}{4}s^2h^2. \quad (3.8)$$

The singlet is charged under a \mathbb{Z}_2 , which restricts the allowed operators, but extends the possible patterns of symmetry breaking, because now $\langle s \rangle = 0$ is radiatively stable. We will focus on a particular parameter region in which there is transitional \mathbb{Z}_2 symmetry breaking: at temperature $T > T_a$ both \mathbb{Z}_2 and the EW symmetry are restored, at $T = T_a$ the singlet obtains a vev breaking \mathbb{Z}_2 , and at $T = T_b < T_a$ the Higgs field obtains a vev and the singlet's vev returns to zero, thereby breaking the EW symmetry and restoring the \mathbb{Z}_2 (i.e., $\text{EW} \times \mathbb{Z}_2 \rightarrow \text{EW} \times \cancel{\mathbb{Z}_2} \rightarrow \text{EW} \times \mathbb{Z}_2$). In the context of this pattern of symmetry breaking, the enhanced discrete symmetry point admits an \mathbb{S}_2 symmetry,

$$\text{EDSP : } b_4 = \lambda \quad \text{and} \quad b_2 = -\mu^2 \quad \mathbb{S}_2 : h \leftrightarrow s \quad (3.9)$$

where we will also take $a_2 > 2\lambda$ to ensure that the discrete symmetry interchanges vacua. Note that this \mathbb{S}_2 symmetry is more restrictive than the \mathbb{Z}_2 symmetries we considered in the previous examples. To illuminate the role of the EDSP in locating SFOPT, we will reparametrize $b_4 = \lambda + \Delta b_4$ and $b_2 = -\mu^2 + \Delta b_2$ to write the potential as

$$U(h, s) = \left[\frac{\lambda}{4}(h^4 + s^4) - \frac{\lambda v^2}{2}(h^2 + s^2) + \frac{a_2}{4}h^2s^2 \right] + \left[\frac{\Delta b_4}{4}s^4 + \frac{\Delta b_2}{2}s^2 \right] \quad (3.10)$$

where we have also used $\mu^2 = \lambda v^2$. In this parameterization, we expect to find SFOPT nearby to the EDSP at $\Delta b_4 = \Delta b_2 = 0$.

We present the results of our numerical analysis in Fig. 4, where we have fixed $\lambda \approx 0.12$ to give a Higgs mass⁴ of $m_h = \sqrt{2\lambda v^2} = 120$ GeV. As in the previous examples, the phase transition strength decreases monotonically with distance from the enhanced symmetry axis. Significantly far from the EDSP, the phase transition proceeds with a different pattern of symmetry breaking. In the brown region, the EW symmetry breaks without transitional \mathbb{Z}_2 violation ($\text{EW} \times \mathbb{Z}_2 \rightarrow \text{EW} \times \mathbb{Z}_2$), in the yellow region the \mathbb{Z}_2 remains broken in the low temperature vacuum ($\text{EW} \times \mathbb{Z}_2 \rightarrow \text{EW} \times \cancel{\mathbb{Z}_2} \rightarrow \text{EW} \times \cancel{\mathbb{Z}_2}$), and in the purple region there exists an intermediate phase in which both \mathbb{Z}_2 and the electroweak symmetry are broken ($\text{EW} \times \mathbb{Z}_2 \rightarrow \text{EW} \times \cancel{\mathbb{Z}_2} \rightarrow \text{EW} \times \cancel{\mathbb{Z}_2} \rightarrow \text{EW} \times \mathbb{Z}_2$).

The region of parameter space nearby to the EDSP displays an interesting phenomenology. Since the singlet mass is given by

$$m_s = m_h \left[\frac{a_2/\lambda}{4} - \frac{1 - \Delta b_2/\lambda v^2}{2} \right]^{1/2} \quad (3.11)$$

one typically finds $m_s \lesssim m_h$ nearby to the enhanced symmetry point. The unbroken \mathbb{Z}_2 symmetry ensures that the singlet is stable, and thus it is a dark matter candidate

⁴Since the axes of Fig. 4 depend only on the ratios $\Delta b_4/\lambda$ and $\Delta b_2/\lambda v^2$, a change in the Higgs mass (via λ) could be absorbed by Δb_4 and Δb_2 , such that the qualitative features of Fig. 4 would remain unchanged.

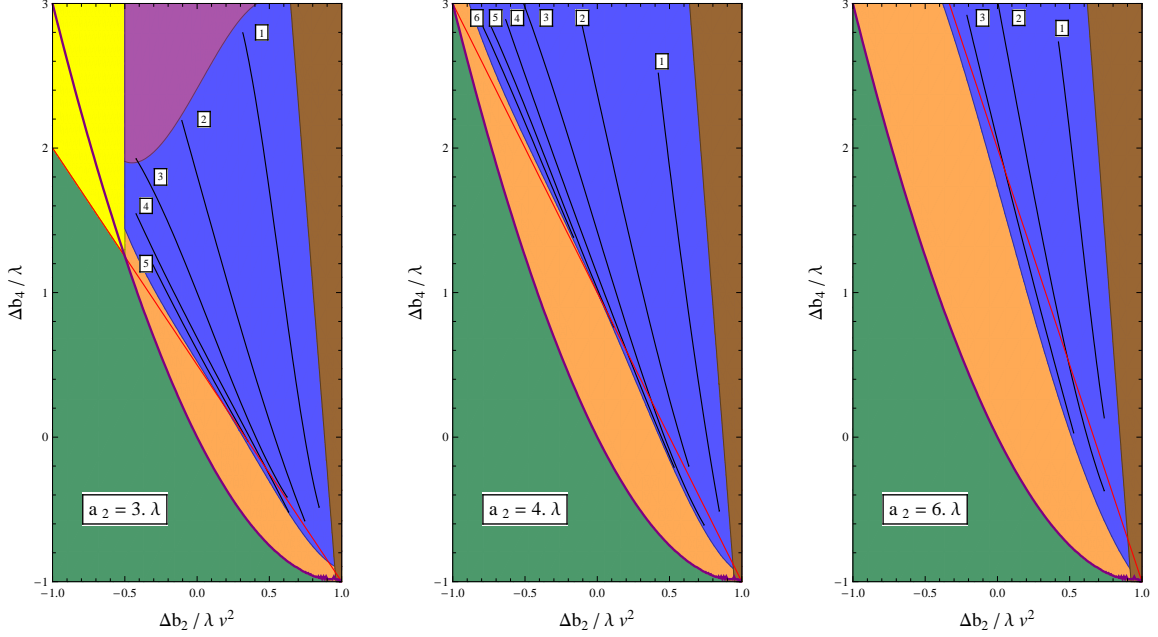


Figure 4. Three slices of the \mathbb{Z}_2 xSM parameter space for fixed $\lambda \approx 0.12$. The origin $\Delta b_2 = \Delta b_4 = 0$ is an EDSP at which the theory has an \mathbb{S}_2 discrete symmetry.

which annihilates to Higgses with a cross section proportional to a_2^2 . A number of analyses [18, 23–30] have considered this scenario and found that a_2 and the singlet mass m_s can be strongly constrained by assuming that the s particle composes all of the dark matter. Collider experiments, such as the LHC, may also be able to constrain the Higgs-singlet coupling. For $\Delta b_2/\lambda v^2 < (3 - a_2/\lambda)/2$, the singlet mass is less than half of the Higgs mass and the invisible decay channel $h \rightarrow ss$ becomes kinematically accessible. Then, a measurement of the invisible decay width may constrain the Higgs-singlet coupling a_2 [17, 30–33]. On the other hand, the singlet self-coupling b_4 remains unconstrained. This is because unlike in other limits of this model and similar models [31, 32, 34], the unbroken \mathbb{Z}_2 symmetry prevents the Higgs and singlet from mixing. Consequently, the singlet self-coupling b_4 is practically impossible to constrain at colliders, and contributions to the anomalous Higgs trilinear coupling [35] are loop suppressed. Finally, let us point out that the transitional \mathbb{Z}_2 violation limit may not suffer from the domain wall problem that generally accompanies models with spontaneously broken discrete symmetries. When the \mathbb{Z}_2 breaks in the first step of the PT, domain walls will be generated. However, once the EW symmetry is broken and the \mathbb{Z}_2 symmetry is restored, the domain walls should be “wiped out” by the \mathbb{Z}_2 -symmetric vacuum field configuration. This may lead to a unique gravitational wave spectrum.

4 Conclusion

Strongly first order phase transitions (SFOPTs) are required for electroweak baryogenesis and may have other interesting implications for early universe relics. In this article we have discussed a general analytic guideline, based on symmetry principles, which is useful in identifying a region of parameter space favorable for SFOPT: an arbitrarily strong PT can be found for parameters near an enhanced discrete symmetry point (EDSP) if the condition for spontaneous symmetry breaking is met and if the discrete symmetry relates the electroweak symmetry preserving vacuum to one in which it is broken. Group theoretically, this means that the coset representation of the broken discrete symmetry contains an electroweak singlet and the discrete group does not commute with the electroweak group. Because of phenomenological requirement of completing the PT at a nonzero temperature, the symmetry must be broken by parametric deformations away from the EDSP. As the deformation decreases, the strength of the PT tends to increase. We applied this guideline to study the electroweak PT in three specific models. In each of the models considered, SFOPTs occur in close proximity to the EDSP, as expected. In this way, the enhanced symmetry point acts like a lamppost in the parameter space, signaling the location of SFOPTs. It would be interesting to apply a similar EDSP-motivated analysis of the electroweak phase transition to models with larger scalar sectors and greater parametric freedom, such as singlet extensions of the Minimal Supersymmetric Standard Model.

We also observe (as did [7, 14]) that the the PT tends not to proceed at all unless the barrier separating the EW-broken and EW-unbroken vacua is very small or not present at all (along the red curve), because otherwise the tunneling rate is too strongly suppressed. Hence, the deformations away from the EDSP required for phenomenologically viable SFOPTs are not vanishingly small and are model dependent. Although such phenomenologically viable parametric regions can be arrived at by deforming away from enhanced continuous symmetry points rather than EDSPs, the EDSP starting point guarantees the existence of potential barriers required for a first order PT. In that sense, our proposal here is advantageous over the enhanced continuous symmetry point perspective.

Proximity to an EDSP implies interesting relations between parameters in the extended Higgs sector, which is responsible for the dynamics of the electroweak symmetry breaking. Such relations will manifest themselves in both the spectrum of the states in the Higgs sector and their couplings. Probing this sector is the central scientific focus of the LHC. We might have already seen the discovery of the Higgs boson on the horizon [36, 37]. Discovering the additional states in the extended Higgs sector and measuring the parameters in the Higgs potential are expected to be very challenging tasks. At the same time, confirming the structure of the Higgs sector to be consistent with a SFOPT would establish a striking link to the generation of the baryonic asymmetry in the universe.

A Details of Phase Transition Calculation

For the phase transition analyses in this paper, we have calculated the thermal effective potential $V_{\text{eff}}(\vec{\phi}, T)$ through one-loop order using the standard techniques [38–40]. We

numerically minimize⁵ V_{eff} with respect to $\vec{\phi}$ to obtain the scalar field expectation values in the symmetric and broken phases, $\vec{v}_{\text{sym}}(T)$ and $\vec{v}_{\text{brk}}(T)$, respectively. The latter quantity is sometimes referred to in the text as simply $v(T)$. The critical temperature T_c is defined as

$$V_{\text{eff}}(\vec{v}_{\text{sym}}(T_c), T_c) = V_{\text{eff}}(\vec{v}_{\text{brk}}(T_c), T_c). \quad (\text{A.1})$$

To determine the bubble nucleation temperature T_n , we use $V_{\text{eff}}(\vec{\phi}, T)$ to calculate the 3D bounce action⁶ $S_3(T)$ [43–46] and solve

$$S_3(T_n)/T_n = 140 \quad (\text{A.2})$$

for T_n [47, 48]. Finally, we calculate the temperature T_r of the plasma after the phase transition ends and the plasma has been reheated. This is obtained by assuming that the universe does not expand significantly during the phase transition and then by imposing energy conservation [6]

$$\rho_{\text{sym}}(T_n) = \rho_{\text{brk}}(T_r) \quad (\text{A.3})$$

where

$$\rho(T) = V_{\text{eff}}(v(T), T) - T \frac{d}{dT} V_{\text{eff}}(v(T), T) \quad (\text{A.4})$$

is the energy density in the symmetric or broken phase, respectively.

Acknowledgments

DJHC thanks Erik Weinberg for an interesting discussion regarding this work at KIAS. Preliminary results of this work were presented by DJHC at “Out-of-Equilibrium Quantum Fields in the Early Universe” in Aachen, September, 2010. DJHC, VB, and AJL were supported in part by the DOE through grant DE-FG02-95ER40896. LTW is supported by the NSF under grant PHY-0756966 and the DOE Early Career Award under grant DE-SC0003930.

References

- [1] V. A. Kuzmin, V. A. Rubakov, and M. E. Shaposhnikov, *On the Anomalous Electroweak Baryon Number Nonconservation in the Early Universe*, *Phys. Lett.* **B155** (1985) 36.
- [2] D. J. Chung and P. Zhou, *Gravity Waves as a Probe of Hubble Expansion Rate During An Electroweak Scale Phase Transition*, *Phys.Rev.* **D82** (2010) 024027, [[arXiv:1003.2462](https://arxiv.org/abs/1003.2462)].

⁵This definition of $v(T)$ implies that T_c , T_n , and T_r will be dependent upon the choice of gauge [41, 42]. Though this may affect the numerical accuracy of our results, we expect that the qualitative parametric dependence of the EW order parameter nearby to an EDSP, which is our primary interest, will remain unchanged.

⁶For the two field models of Secs. 3.2 and 3.3 we calculate the bounce using the approximation described in [6].

- [3] S. J. Huber and T. Konstandin, *Gravitational Wave Production by Collisions: More Bubbles*, *JCAP* **0809** (2008) 022, [[arXiv:0806.1828](#)].
- [4] C. Caprini, R. Durrer, and G. Servant, *The stochastic gravitational wave background from turbulence and magnetic fields generated by a first-order phase transition*, *JCAP* **0912** (2009) 024, [[arXiv:0909.0622](#)]. * Brief entry *.
- [5] T. Kahniashvili, L. Kisslinger, and T. Stevens, *Gravitational Radiation Generated by Magnetic Fields in Cosmological Phase Transitions*, *Phys.Rev.* **D81** (2010) 023004, [[arXiv:0905.0643](#)].
- [6] D. J. Chung and A. J. Long, *Cosmological Constant, Dark Matter, and Electroweak Phase Transition*, [arXiv:1108.5193](#). * Temporary entry *.
- [7] D. Chung, A. Long, and L.-T. Wang, *Probing the Cosmological Constant and Phase Transitions with Dark Matter*, *Phys.Rev.* **D84** (2011) 043523, [[arXiv:1104.5034](#)].
- [8] C. Wainwright and S. Profumo, *The Impact of a Strongly First-Order Phase Transition on the Abundance of Thermal Relics*, *Phys. Rev.* **D80** (2009) 103517, [[arXiv:0909.1317](#)].
- [9] T. Cohen, D. E. Morrissey, and A. Pierce, *Changes in Dark Matter Properties After Freeze-Out*, *Phys. Rev.* **D78** (2008) 111701, [[arXiv:0808.3994](#)].
- [10] F. R. Klinkhamer and N. S. Manton, *A Saddle Point Solution in the Weinberg-Salam Theory*, *Phys. Rev.* **D30** (1984) 2212.
- [11] F. Csikor, Z. Fodor, and J. Heitger, *Endpoint of the hot electroweak phase transition*, *Phys. Rev. Lett.* **82** (1999) 21–24, [[hep-ph/9809291](#)].
- [12] T. Kibble, *Topology of Cosmic Domains and Strings*, *J.Phys.A* **A9** (1976) 1387–1398.
- [13] A. Vilenkin and E. Shellard, *Cosmic strings and other topological defects*. Cambridge monographs on mathematical physics. Cambridge University Press, 2000.
- [14] J. R. Espinosa, T. Konstandin, and F. Riva, *Strong Electroweak Phase Transitions in the Standard Model with a Singlet*, *Nucl.Phys.* **B854** (2012) 592–630, [[arXiv:1107.5441](#)].
- [15] C. Grojean, G. Servant, and J. D. Wells, *First-order electroweak phase transition in the standard model with a low cutoff*, *Phys. Rev.* **D71** (2005) 036001, [[hep-ph/0407019](#)].
- [16] C. Delaunay, C. Grojean, and J. D. Wells, *Dynamics of Non-renormalizable Electroweak Symmetry Breaking*, *JHEP* **04** (2008) 029, [[arXiv:0711.2511](#)].
- [17] V. Barger, T. Han, P. Langacker, B. McElrath, and P. Zerwas, *Effects of genuine dimension-six Higgs operators*, *Phys.Rev.* **D67** (2003) 115001, [[hep-ph/0301097](#)].
- [18] V. Barger, P. Langacker, M. McCaskey, M. J. Ramsey-Musolf, and G. Shaughnessy, *LHC Phenomenology of an Extended Standard Model with a Real Scalar Singlet*, *Phys. Rev.* **D77** (2008) 035005, [[arXiv:0706.4311](#)].
- [19] S. Profumo, M. J. Ramsey-Musolf, and G. Shaughnessy, *Singlet Higgs Phenomenology and the Electroweak Phase Transition*, *JHEP* **08** (2007) 010, [[arXiv:0705.2425](#)].
- [20] S. W. Ham, Y. S. Jeong, and S. K. Oh, *Electroweak phase transition in an extension of the standard model with a real Higgs singlet*, *J. Phys.* **G31** (2005) 857–872, [[hep-ph/0411352](#)].
- [21] A. Ahriche, *What is the Criterion for a Strong First Order Electroweak Phase Transition in Singlet Models?*, *Phys. Rev.* **D75** (2007) 083522, [[hep-ph/0701192](#)].
- [22] S. Profumo, L. Ubaldi, and C. Wainwright, *Singlet Scalar Dark Matter: monochromatic*

- gamma rays and metastable vacua*, *Phys.Rev.* **D82** (2010) 123514, [[arXiv:1009.5377](#)].
- [23] M. Gonderinger, Y. Li, H. Patel, and M. J. Ramsey-Musolf, *Vacuum Stability, Perturbativity, and Scalar Singlet Dark Matter*, *JHEP* **01** (2010) 053, [[arXiv:0910.3167](#)].
- [24] J. McDonald, *Gauge Singlet Scalars as Cold Dark Matter*, *Phys. Rev.* **D50** (1994) 3637–3649, [[hep-ph/0702143](#)].
- [25] C. P. Burgess, M. Pospelov, and T. ter Veldhuis, *The Minimal Model of Nonbaryonic Dark Matter: A Singlet Scalar*, *Nucl. Phys.* **B619** (2001) 709–728, [[hep-ph/0011335](#)].
- [26] X.-G. He, T. Li, X.-Q. Li, and H.-C. Tsai, *Scalar Dark Matter Effects in Higgs and Top Quark Decays*, *Mod. Phys. Lett.* **A22** (2007) 2121–2129, [[hep-ph/0701156](#)].
- [27] H. Davoudiasl, R. Kitano, T. Li, and H. Murayama, *The New Minimal Standard Model*, *Phys. Lett.* **B609** (2005) 117–123, [[hep-ph/0405097](#)].
- [28] A. Bandyopadhyay, S. Chakraborty, A. Ghosal, and D. Majumdar, *Constraining Scalar Singlet Dark Matter with CDMS, XENON and DAMA and Prediction for Direct Detection Rates*, *JHEP* **11** (2010) 065, [[arXiv:1003.0809](#)].
- [29] T. Cohen, J. Kearney, A. Pierce, and D. Tucker-Smith, *Singlet-Doublet Dark Matter*, [arXiv:1109.2604](#). * Temporary entry *.
- [30] I. Low, P. Schwaller, G. Shaughnessy, and C. E. Wagner, *The dark side of the Higgs boson*, [arXiv:1110.4405](#).
- [31] C. Englert, T. Plehn, D. Zerwas, and P. M. Zerwas, *Exploring the Higgs portal*, *Phys.Lett.* **B703** (2011) 298–305, [[arXiv:1106.3097](#)].
- [32] S. Bock, R. Lafaye, T. Plehn, M. Rauch, D. Zerwas, *et. al.*, *Measuring Hidden Higgs and Strongly-Interacting Higgs Scenarios*, *Phys.Lett.* **B694** (2010) 44–53, [[arXiv:1007.2645](#)].
- [33] C. Englert, T. Plehn, M. Rauch, D. Zerwas, and P. M. Zerwas, *LHC: Standard Higgs and Hidden Higgs*, [arXiv:1112.3007](#).
- [34] A. Noble and M. Perelstein, *Higgs Self-Coupling as a Probe of Electroweak Phase Transition*, *Phys. Rev.* **D78** (2008) 063518, [[arXiv:0711.3018](#)].
- [35] A. Djouadi, W. Kilian, M. Muhlleitner, and P. Zerwas, *Production of neutral Higgs boson pairs at LHC*, *Eur.Phys.J.* **C10** (1999) 45–49, [[hep-ph/9904287](#)].
- [36] *Combination of Higgs Boson Searches with up to 4.9 fb⁻¹ of p p Collision Data Taken at sqrt(s)=7 TeV with the ATLAS Experiment at the LHC*, The ATLAS collaboration, ATLAS-CONF-2011-163.
- [37] *Combination of CMS searches for a Standard Model Higgsboson*, The CMS collaboration, CMS PAS HIG-11-032.
- [38] S. R. Coleman and E. Weinberg, *Radiative Corrections as the Origin of Spontaneous Symmetry Breaking*, *Phys. Rev.* **D7** (1973) 1888–1910.
- [39] L. Dolan and R. Jackiw, *Symmetry Behavior at Finite Temperature*, *Phys. Rev.* **D9** (1974) 3320–3341.
- [40] R. Jackiw, *Functional evaluation of the effective potential*, *Phys. Rev.* **D9** (1974) 1686.
- [41] H. H. Patel and M. J. Ramsey-Musolf, *Baryon Washout, Electroweak Phase Transition, and Perturbation Theory*, [arXiv:1101.4665](#).
- [42] W. Loinaz and R. S. Willey, *Gauge dependence of lower bounds on the Higgs mass derived*

- from electroweak vacuum stability constraints, *Phys. Rev.* **D56** (1997) 7416–7426, [[hep-ph/9702321](#)].
- [43] A. D. Linde, *On the Vacuum Instability and the Higgs Meson Mass*, *Phys. Lett.* **B70** (1977) 306.
- [44] A. D. Linde, *Decay of the False Vacuum at Finite Temperature*, *Nucl. Phys.* **B216** (1983) 421.
- [45] S. R. Coleman, *The Fate of the False Vacuum. 1. Semiclassical Theory*, *Phys. Rev.* **D15** (1977) 2929–2936.
- [46] C. G. Callan and S. R. Coleman, *The Fate of the False Vacuum. 2. First Quantum Corrections*, *Phys. Rev.* **D16** (1977) 1762–1768.
- [47] L. D. McLerran, M. E. Shaposhnikov, N. Turok, and M. B. Voloshin, *Why the baryon asymmetry of the universe is approximately $10^{*}-10$* , *Phys. Lett.* **B256** (1991) 477–483.
- [48] G. W. Anderson and L. J. Hall, *The Electroweak phase transition and baryogenesis*, *Phys. Rev.* **D45** (1992) 2685–2698.